https://doi.org/10.1016/j.applthermaleng.2021.117857


# Flow Measurement Uncertainty Quantification for Building Central Cooling Systems with Multiple Water-Cooled Chillers Using a Bayesian Approach

Shaobo Sun [1], Shengwei Wang [1,2] * and Kui Shan [1,2]

[1] Department of Building Environment and Energy Engineering, [2] Research Institute for Smart Energy

The Hong Kong Polytechnic University, Kowloon, Hong Kong

**Abstract:** Measurement uncertainty has significant negative impacts on the operation and control of heating, ventilation and air conditioning systems. It is a big challenge and should be solved urgently. Existing studies focus on reducing the impacts of measurement uncertainty by developing uncertainty tolerant methods without quantifying the measurement uncertainties themselves. They therefore fail to fundamentally solve them. This study aims to directly quantify the measurement uncertainties of water flow meters in multiple water-cooled chiller systems using a Bayesian approach. A measurement uncertainty quantification strategy is proposed based on Bayesian inference and energy balance models, and the Markov chain Monto Carlo method is used to achieve the strategy. The site data collected from a chiller system are used to test the strategy. Four simulation tests with different levels of measurement uncertainty are conducted to further test and systematically validate the strategy. Test results show that the measurement uncertainties (both systematic and random uncertainties) of the water flow meters in the chiller systems can be quantified effectively and with acceptable accuracy. The strategy performs very well in quantifying random uncertainties of flow meters, and the relative errors range from 0% to 12.8%. The performance of the strategy in quantifying systematic uncertainties is also satisfactory, and the relative errors range from 0.1% to 36.57%. The proposed strategy is able to quantify measurement uncertainties and can be used to optimize the control of chiller systems and improve the reliability of chiller systems.

**Keywords:** Measurement uncertainty, uncertainty quantification, Bayesian inference, chiller system, water flow meter.

* *Corresponding author: Shengwei Wang, email: beswwang@polyu.edu.hk*

**Nomenclature**

| | |
|---|---|
| *HVAC* | heating, ventilation and air conditioning |
| *MCMC* | Markov chain Monte Carlo |
| *NUTS* | No-U-Turn Sampler |
| *HMC* | Hamiltonian Monte Carlo |
| *cLHS* | conditioned Latin hypercube sampling |
| *CHWFM* | chilled water flow meter |
| *CWFM* | cooling water flow meter |
| $K$ | number of warmup iterations/samples |
| $P$ | power consumption of chiller (kW) |
| $T$ | temperature (°C) |
| $q$ | true volumetric flow rate of water (L/s) |
| $\tilde{q}$ | measured volumetric flow rate of water (L/s) |
| $\bar{q}$ | mean of true volumetric water flow rate (L/s) |
| $u$ | measurement uncertainty |
| $N_{chain}$ | number of Markov chains |
| $N_{iter}$ | number of iterations |
| $q_r$ | rated flow rate of water pump (L/s) |
| $q_{ref}$ | reference value of water flow rate under actual working condition (L/s) |
| $Q_{in}$ | heat absorption of evaporator in chiller (kW) |
| $Q_{out}$ | heat rejection of condenser in chiller (kW) |
| $c$ | specific heat capacity of water (kJ/(kg·°C)) |
| $n$ | number of chillers |
| *COP* | coefficient of performance |
| $COP_{FL}$ | full load coefficient of performance |
| *CP* | cooling capacity of chiller (kW) |
| $r_p$ | part load ratio of chiller |

*Greek letters*

| | |
|---|---|
| $\rho$ | density of water (kg/m$^3$) |
| $\mu$ | systematic uncertainty of flow meter (L/s) |
| $\sigma$ | standard deviation of random uncertainty of flow meter |
| $\alpha$ | ratio of actual (part-load) COP of chiller to its full load COP |
| $\delta$ | standard deviation of true volumetric water flow rate |

*Subscripts*

| | |
|---|---|
| *chw* | chilled water |
| *chws* | chilled water supply |
| *chwr* | chilled water return |
| *cw* | cooling water |
| *cwin* | cooling water inlet |
| *cwout* | cooling water outlet |
| *chwq* | chilled water flow meter |
| *cwq* | cooling water flow meter |
| *i* | chiller No. |

## 1. Introduction

In order to provide cooling or heating to indoor spaces and guarantee indoor thermal comfort, almost all modern buildings are equipped with heating, ventilation and air conditioning (HVAC) systems. They are major energy consumers in most buildings. The building sector consumes about 40% of end-use energy [1], and the electricity consumed by HVAC systems accounts for over 50% of total building electricity use [2]. In order to improve the overall energy efficiency of HVAC systems and reduce energy waste, many researchers have tried to develop optimal control strategies for HVAC systems. Karami and Wang [3] employed the particle swarm optimization search algorithm to optimize the chilled water temperature setpoint, condenser water temperature setpoint and threshold of cooling load during the chiller stage sequence for a multiple-chiller plant with non-identical chillers. Mu et al. [4] proposed a model-free optimization strategy based on multivariate extremum seeking control with penalty terms to maximize the energy efficiency of a chilled-water plant with parallel chillers. Teimourzadeh et al. [5] optimized cooling-load dispatch for multiple-chiller plants through an augmented group search optimization algorithm. There is no doubt that control strategies for HVAC systems are becoming more and more precise due to the efforts of researchers.

However, no matter how good the control strategy is, its implementation must rely on one or more measurements. Measurement uncertainty cannot be avoided regardless of how accurate the sensors used are, and it may lead to significant negative impacts on system control, energy consumption, indoor thermal comfort, etc. Existing studies show that energy consumption increases by 17% in cooling mode and 43% in heating mode due to the measurement uncertainties in outdoor air flow control [6]. Uncertainties in occupancy measurements can lead to an 18% and 16.5% increase in total energy consumption in winter and summer days respectively [7]. Liao et al. [8] systematically analysed the impacts of uncertainties on four typical chiller sequencing control strategies, results show that uncertainties affected the chiller switching frequency, supply air temperature and energy consumption. Generally, sensors should be calibrated annually [9], but it is in fact very difficult to carry out field calibration for sensors. As a result, many sensors are never calibrated in their life cycles. In addition, even if the sensors are calibrated, the calibration interval is usually long, and so the impacts of measurement uncertainties cannot be reduced to an acceptable level. Hence, in order to reduce the impacts of measurement uncertainties on the operation of HVAC systems, researchers have proposed control strategies which can tolerate or remove a certain level of measurement

uncertainties. Zhuang et al. [10, 11] proposed a risk-based robust optimal control strategy to deal with measurement uncertainties. Huang et al. [12] reduced measurement uncertainties by fusing available redundant measurements while considering outliers, noises and biases in order to improve cooling load measurement. Sun et al. [13] utilized fused measurements to deal with possible misbehaviours in measurement instruments. Shi et al. [14] proposed an exergy-analysis-based method to evaluate the energy saving potential of HVAC systems under measurement uncertainties. Yang et al. [15] presented an online fault-tolerate control strategy to correct faulty measurements. These studies all addressed measurement uncertainties indirectly: they aimed to reduce their impacts rather than quantify them directly. In other words, the measurement uncertainties have not fundamentally been solved.

According to the ISO/IEC GUIDE 98-3 [16], the measurement uncertainty considered in this study is a Type B uncertainty, because the uncertainty is not evaluated by the statistical analysis of series of observations. In this study, the measurement uncertainty (including the measuremen error) is divided into two components: a systematic uncertainty (also known as bias) and a random uncertainty (also known as noise). The systematic uncertainty is generally considered to be fixed or varying very slowly over time. The random uncertainty is of course random but can be considered to generally follow a normal distribution. Some studies only consider the random uncertainties of measurements without taking the systematic uncertainties into account. In fact, both systematic and random uncertainties may lead to negative effects and cannot be ignored. In addition, the focus of most existing studies is the effects of measurement uncertainties on the operation and control of HVAC systems instead of the measurement uncertainties themselves. There are very few studies on quantifying both systematic and random uncertainties of measurements directly. It is a big challenge to quantify measurement uncertainty directly. Fortunately, Bayesian inference, a powerful uncertainty analysis method, can provide a means to cope with this challenge.

Bayesian techniques have commonly been used for inverse uncertainty quantification in building energy models [17]. The purpose of inverse uncertainty quantification is to estimate the unknown variables in building energy models using mathematical formulations [18] and observational data. It is also called model calibration. There are many successful application cases of Bayesian theory in model calibration. For example, Heo et al. [19] calibrated normative energy models with a Bayesian approach to evaluate different energy retrofit options. Chong et al. [20] validated the ability of Bayesian calibration using two different building energy models. Booth et al. [21] used Bayesian calibration to handle uncertainties in housing stock models. Moreover, Bayesian inference can be used in conjunction with machine learning

algorithms. Liu et al. [22, 23] used feedforward neural network, principal component analysis and Gaussian process to develop the surrogate models and enhanced the computational efficiency of Bayesian-based uncertainty quantification significantly. Zhu et al. [24] used support vector machine and neural network to extend the application of an approximate Bayesian computation method in the calibration of building energy models. Burkhart [25] and Heo [26] used a Bayesian-based Gaussian process modelling framework to handle uncertainties in measurement and verification practices. Similarly, the kind of measurement uncertainty quantification concerned in this study can also be considered an inverse problem. It is possible to estimate unknown systematic and random uncertainties using available measurements. Moreover, the energy balance models, as an inherent correlation between measurements, can be used as constraints to improve quantification accuracy.

Therefore, this study aims to directly quantify measurement uncertainties of water flow meters in chiller systems. Due to high flexibility [27], multiple water-cooled chiller systems are widely used in large-scale commercial buildings, and a typical multiple water-cooled chiller system is selected as the reference system for this study. A measurement uncertainty quantification strategy based on Bayesian inference and energy balance models is proposed. The measurement uncertainties (both systematic and random uncertainties) of flow meters in the chiller system are considered. The main innovation of this strategy is that the measurement uncertainties are quantified directly, including both systematic and random uncertainties of measurements. The proposed strategy can be used for online sensor calibration, significantly reducing the costs. It can also enhance the robustness of decision-making schemes for the control of HVAC systems.

## 2. Multiple water-cooled chiller systems and measurement uncertainties

### *2.1 System description*

A multiple water-cooled chiller system typically consists of a chilled water system and a cooling water system, as shown in Fig. 1. The chilled water loop connects the chillers with the building. The cooling water loop connects the chillers with the cooling towers. Each chiller is interlocked with a constant-speed chilled water pump on the water return side and a constant-speed cooling water pump on the water inlet side. A number of temperature sensors, chilled water flow meters (CHWFM), cooling water flow meters (CWFM), power meters, etc., are installed in the system for system monitoring and online real-time control. For each chiller, the power consumption ($P_i$), chilled water supply temperature ($T_{chws,i}$) and return temperature

($T_{chwr,i}$), chilled water volume flow rate ($q_{chw,i}$), cooling water inlet temperature ($T_{cwin,i}$) and outlet temperature ($T_{cwout,i}$), and cooling water volume flow rate ($q_{cw,i}$) are measured. On the main pipe, the main chilled water supply temperature ($T_{chws}$) and return temperature ($T_{chwr}$), main chilled water volume flow rate ($q_{chw}$), main cooling water inlet temperature ($T_{cwin}$) and outlet temperature ($T_{cwout}$), and main cooling water volume flow rate ($q_{cw}$) are also measured.

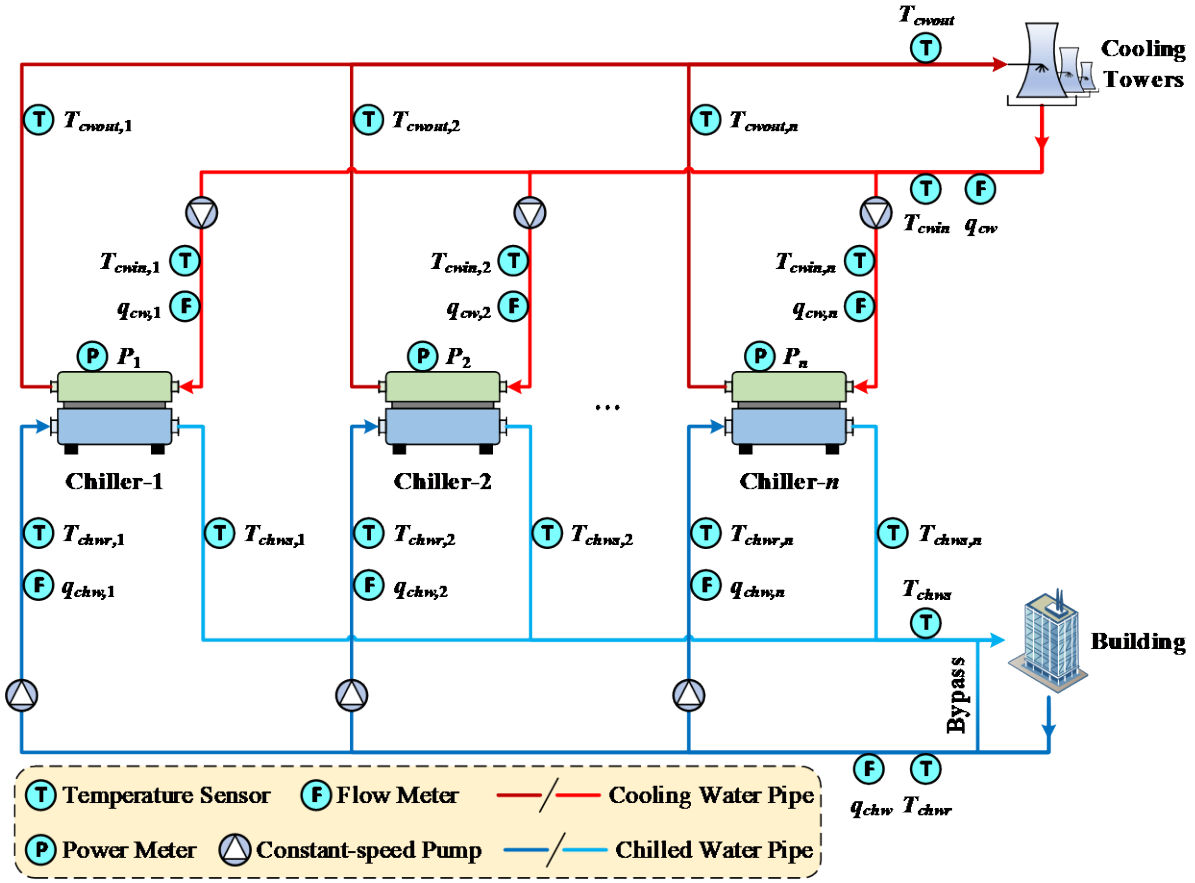


Fig. 1. Schematic of a multiple water-cooled chiller system and metering arrangement

### *2.2 Basic characteristics of measurement uncertainty*

The measured values ($\tilde{x}$) of a variable can be divided into two parts as shown in Eq. (1), i.e. the true values ($x$) and an uncertain term ($u_x$). The true values can never be determined exactly. In this study, the uncertain term represents measurement uncertainty and can be considered to follow a normal distribution with mean $\mu_x$ and standard deviation $\sigma_x$, as shown in Eq. (2). Its mean represents the systematic uncertainty of measurement, and its standard deviation reflects the random uncertainty of measurement. According to the characteristics of a normal distribution, the actual measured values of the variable also follow a normal distribution with mean ($x + \mu_x$) and standard deviation $\sigma_x$, as shown in Eq. (3).

$$\tilde{x} = x + u_x \tag{1}$$

$$\boldsymbol{u}_x \sim \boldsymbol{N}\left(\mu_x,\ \sigma_x^2\right) \tag{2}$$

$$\tilde{\boldsymbol{x}} \sim \boldsymbol{N}\left(\boldsymbol{x}+\mu_x,\ \sigma_x^2\right) \tag{3}$$

As mentioned before, temperature sensors, flow meters, power meters, etc., are all installed in the chiller systems. The measurement uncertainties of these sensors are unavoidable. In this study, only the measurement uncertainties of water flow meters are considered for the following reasons: (1) The computation load will increase significantly if uncertainties of more sensors are included in quantification; (2) Temperature sensors can be calibrated using other relatively easier means compared with water flow meters, and the cost of replacing temperature sensors is much lower than that for flow meters; (3) Power meters have higher accuracy and are easier to calibrate.

## 3. Measurement uncertainty quantification strategy

### *3.1 The basic approach and procedure*

Uncertainty exists inherently in all measurements and determines measurement quality as well as the accuracy and reliability of decisions made using the measurements. Quantification of measurement uncertainty is therefore an essential means to ensure or improve the accuracy and reliability of decisions. Fig. 2 shows the basic procedure of measurement uncertainty quantification proposed in this study. A key feature is that the measurements are the only inputs needed. The tool used in this study is the *Stan* programming language. The number of Markov chains ($N_{chain}$) is set to 4 by default. In order to reduce computational load, the number of iterations ($N_{iter}$) should be set as small as possible while ensuring that the chains can converge to the same value. The parameter *Rhat* is used to check convergence. If the chains have converged, *Rhat* will near 1. Otherwise, *Rhat* will be larger than 1. In general, it is acceptable for *Rhat* to be no more than 1.01 [28]. Apart from *Rhat*, the traces and autocorrelations of samples are also used for checking whether the Markov chains are converged in this study [29]. Based on these criterions, the number of iterations can be set properly. In addition, it is necessary to assign a prior distribution to the uncertainty of each measurement - the details will be provided in Section 3.3. The Markov chain Monte Carlo (MCMC) method is used to generate samples under the constraints of the energy balance models. During the iterative process, prior distributions are updated continually, and the posterior distributions are calculated using the generated samples and measurement uncertainty models (i.e. likelihoods) according to Bayes' theorem. The posterior distributions are the outputs of the uncertainty

quantification and show the possible distributions of unknown uncertainties. The methods and models used will be introduced in detail in the following sections.

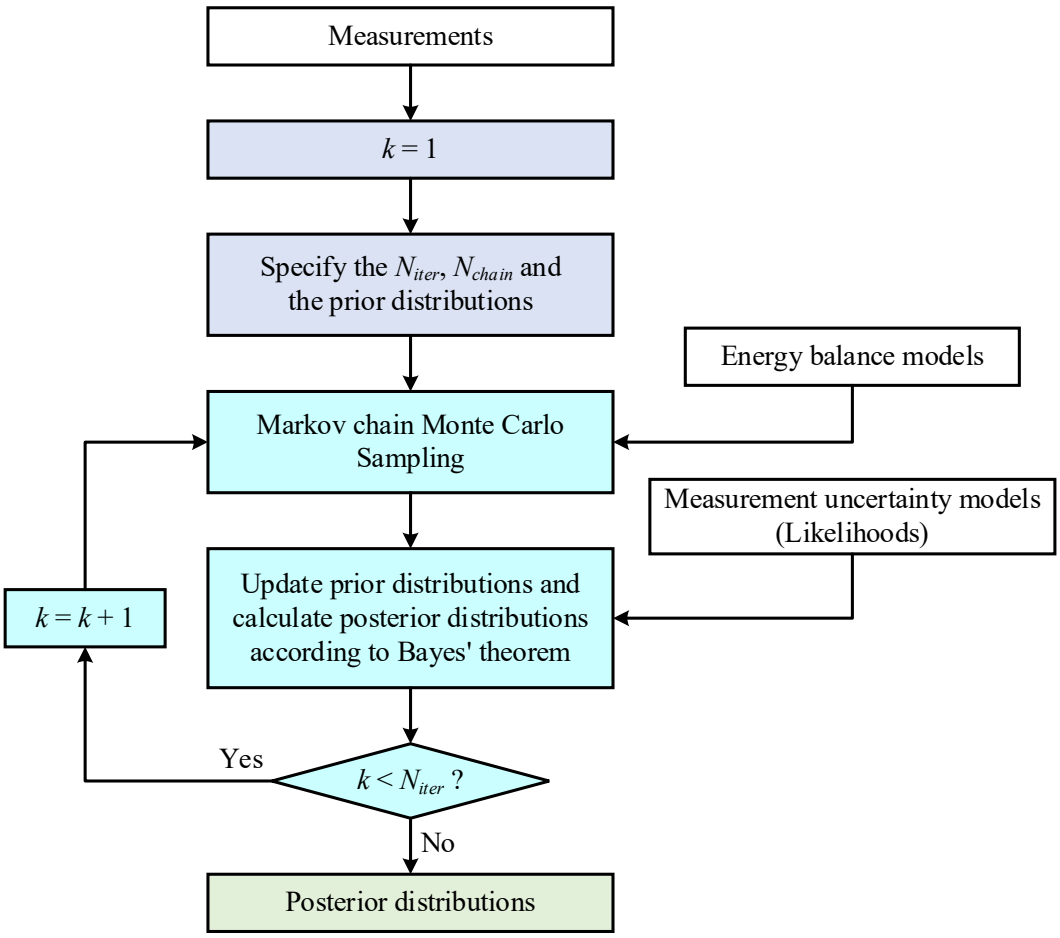


Fig. 2. Basic procedure of measurement uncertainty quantification

### *3.2 Measurement uncertainty quantification methods adopted*

Two advanced methods, Bayesian inference and No-U-Turn Sampler (NUTS), are adopted in the measurement uncertainty quantification strategy. An outline of these two methods is given below.

#### *3.2.1 Bayesian inference*

Bayesian inference utilizes prior distribution and likelihood function to compute the posterior distribution according to Bayes' theorem. The mathematical formulation of Bayes' theorem is stated as Eq. (4).

$$p(\theta \mid y) = \frac{p(y \mid \theta) \cdot p(\theta)}{p(y)} \propto p(y \mid \theta) \cdot p(\theta) \tag{4}$$

Where, $\theta$ represents the unknown parameters to be estimated, $y$ is the observational data, $p(\theta|y)$ is the posterior probability, $p(y|\theta)$ is the likelihood function, $p(\theta)$ is the prior

probability, and $p(y)$ is the marginal likelihood. The posterior probability is proportional to the prior probability multiplied by the likelihood function. The prior probability is the inherent likeliness and reflects the beliefs about $\theta$ without considering the observational data, while the posterior probability signifies the beliefs about $\theta$ considering observational data. The posterior probability is calculated using the likelihood function and observational data according to Bayes' theorem, and is mainly affected by the prior probability and the likelihood function.

*3.2.2 No-U-Turn Sampler (NUTS)*

Monte Carlo method can achieve the propagation of distributions and is effective to explore the distributions of unknown uncertainties [30]. The proposed strategy adopts the MCMC sampling method to realize Bayesian inference and quantify the measurement uncertainties. The MCMC sampling method is commonly used to compute the posterior distribution in Bayesian analysis, it can draw samples from high-dimensional posterior distributions [31]. Although there are many kinds of MCMC algorithms, most of them are plagued by random walk behaviour and are sensitive to correlated parameters. The Hamiltonian Monte Carlo (HMC) method is one of the most popular MCMC algorithms and can avoid the above issues by taking a series of steps based on first-order gradient information [32]. However, the performance of HMC is heavily dependent on two main parameters: the leapfrog step size and the number of leapfrog steps per iteration [20]. Hoffman and Gelman [33] extended the HMC algorithm and proposed the No-U-Turn Sampler (NUTS) to solve the problem. NUTS can search for the number of leapfrog steps automatically using a recursive algorithm and can adapt the leapfrog step size using a primal-dual averaging scheme. Not only does NUTS not require user intervention or costly tuning runs, but it also performs at least as well as HMC method. Therefore, this study uses the NUTS method to generate samples for computing the posterior distributions of unknown parameters in Bayesian inference.

### *3.3 Prior distributions*

In order to estimate the unknown variables and measurement uncertainties, prior distributions must be assigned to each of them. In general, prior distributions can be derived from expert knowledge, experiments, surveys and industrial standards, among other sources [19]. In this study, the unknown variables include the true water flow rates, while the measurement uncertainties include the systematic uncertainty (i.e. $\mu_x$ in Eq. (2)) and random uncertainty of each flow meter. A normal distribution is chosen as the prior distribution of systematic uncertainty. Its mean is set to 0 because the systematic uncertainty can be positive

or negative. Its standard deviation is determined through the hypothesis that the probability of the systematic uncertainty being less than 10% of the rated flow rate ($q_r$) is 95%, as shown in Fig. 3. Therefore, the prior distributions of the systematic uncertainties can be determined once the rated flow rates of the corresponding water pumps are determined.

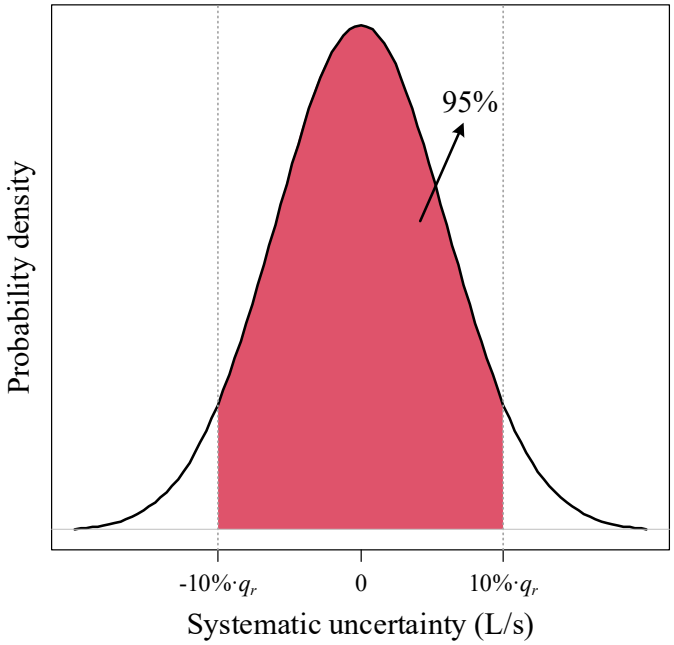


Fig. 3. Prior distribution of systematic uncertainty

The random uncertainty of each flow meter is not fixed and can be represented by its standard deviation (i.e. $\sigma_x$ in Eq. (2)). As it is well-known that standard deviation must be greater than 0, the chi-square distribution with 3 degrees of freedom ($\chi^2(3)$) is assigned to be the prior distributions of random uncertainty of each flow meter, as shown in Fig. 4.

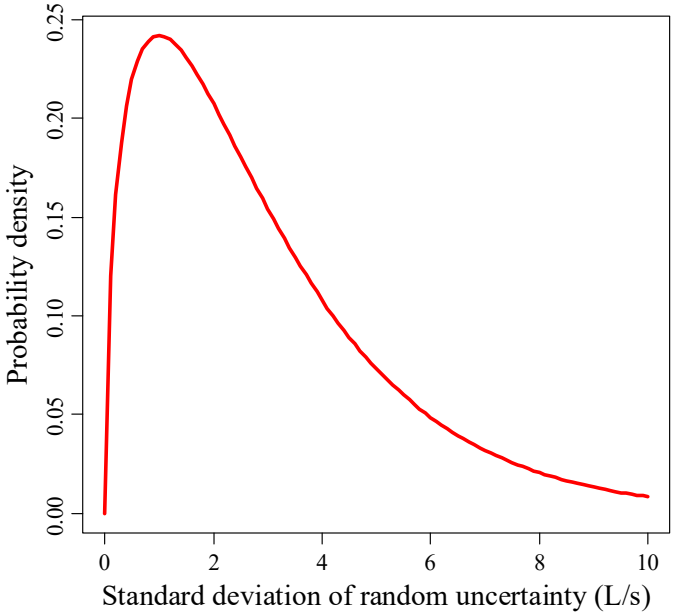


Fig. 4. Prior distribution of random uncertainty

In order to quantify the measurement uncertainties of flow meters more accurately, further information about the true water flow rates is considered. Because both chilled water and cooling water are driven by constant-speed pumps, their flow rates may follow normal distributions as shown in Eq. (5) and (6). However, the means and standard deviations of these distributions are unknown. In principle, the water flow rate can be determined by the pump head according to the characteristic curve of the pump concerned. The pump head can be measured on-site. The flow rate corresponding to the measured pump head on the characteristic curve of the pump is then the reference value of the true water flow rate (denoted by $q_{ref}$). In reality, the mean of the true water flow rate may deviate from $q_{ref}$, due to the actual pressure heads as well as other factors. The prior distributions of the means of the chilled water flow rates ($\bar{q}_{chw,i}$) and cooling water flow rates ($\bar{q}_{cw,i}$) can be assigned by referring to the assignment of prior distribution of systematic uncertainty. In this study, it is assumed that the probability that the mean deviates from $q_{ref}$ by less than 3% is 95%, as shown in Fig. 5.

$$\boldsymbol{q}_{chw,i} \sim N\left(\bar{q}_{chw,i}, \delta^2_{chw,i}\right), \quad i = 1,2,...,n \tag{5}$$

$$\boldsymbol{q}_{cw,i} \sim N\left(\bar{q}_{cw,i}, \delta^2_{cw,i}\right), \quad i = 1,2,...,n \tag{6}$$

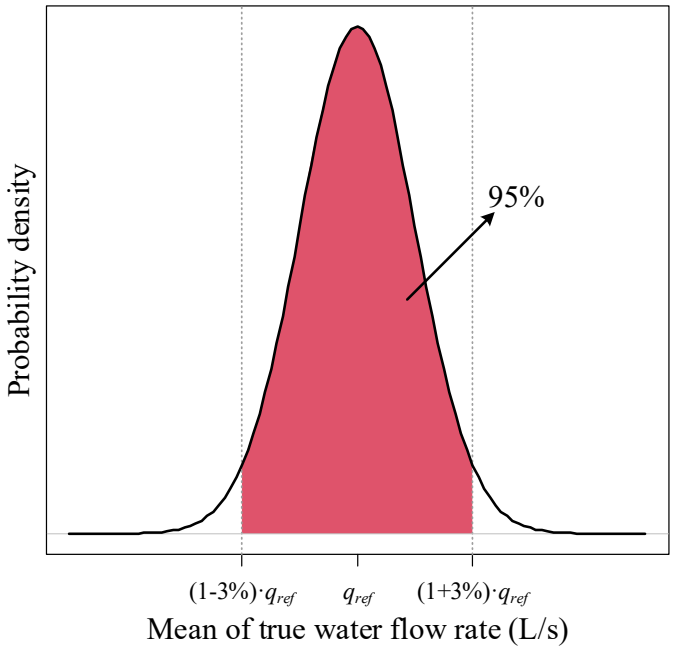


Fig. 5. Prior distribution of the mean of true water flow rate

### *3.4 Energy balance models*

As mentioned previously, many variables are measured in real time. In principle, there are certain numerical relationships between these variables, as they should obey basic rules such as energy and mass balance. Fig. 6 shows the principle of a water-cooled chiller (Chiller-*i*). The heat is transferred from the chilled water to the cooling water indirectly by a vapor compression refrigeration cycle, as shown in Fig. 6 (a). As a medium of heat transfer, the refrigerant absorbs the heat of chilled water and discharges the heat to cooling water. The refrigerant goes through a compression process (1→2), a condensation process (2→3→4), a throttling process (4→5) and an evaporation process (5→1) to complete a cycle. The state of the refrigerant during the cycle can be presented in the pressure-enthalpy (*p*-*h*) and temperature-entropy (*T*-*s*) diagrams, as shown in Fig. 6 (b) and (c). According to the law of energy balance, the input power of the compressor ($P_i$) plus the heat absorption of the evaporator ($Q_{in,i}$) equals the heat rejection of the condenser ($Q_{out,i}$), as shown in Eq. (7). Where, $c$ is the specific heat capacity of water ($kJ/(kg \cdot ℃)$), and $\rho$ is the density of water ($kg/m^3$).

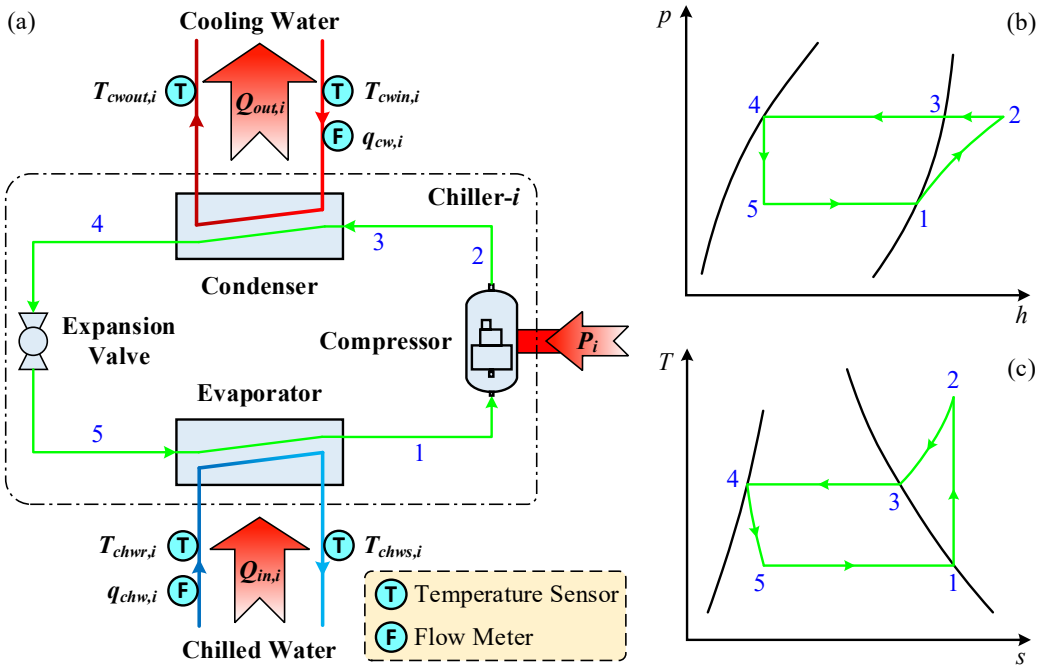


Fig. 6. Principle of a water-cooled chiller (Chiller-*i*): (a) Schematic diagram, (b) *p*-*h* diagram, (c) *T*-*s* diagram

$$\begin{cases} \boldsymbol{P}_i + \boldsymbol{Q}_{in,i} = \boldsymbol{Q}_{out,i} \\ \boldsymbol{Q}_{in,i} = c \cdot \rho \cdot \boldsymbol{q}_{chw,i} \cdot \left( \boldsymbol{T}_{chwr,i} - \boldsymbol{T}_{chws,i} \right), \quad i = 1,2,...,n \\ \boldsymbol{Q}_{out,i} = c \cdot \rho \cdot \boldsymbol{q}_{cw,i} \cdot \left( \boldsymbol{T}_{cwout,i} - \boldsymbol{T}_{cwin,i} \right) \end{cases} \tag{7}$$

In addition, in a multiple water-cooled chiller system, the chilled water from each chiller mixes into the main supply pipe, which should also satisfy the law of energy and mass balance, as shown in Eq. (8) and Eq. (9). Similarly, the mixing of cooling water from each chiller should satisfy Eq. (10) and Eq. (11). These equations are used to constrain the MCMC sampling in this study.

$$\boldsymbol{T}_{chws} \cdot \boldsymbol{q}_{chw} = \boldsymbol{T}_{chws,1} \cdot \boldsymbol{q}_{chw,1} + \boldsymbol{T}_{chws,2} \cdot \boldsymbol{q}_{chw,2} + \cdots + \boldsymbol{T}_{chws,n} \cdot \boldsymbol{q}_{chw,n} \tag{8}$$

$$\boldsymbol{q}_{chw} = \boldsymbol{q}_{chw,1} + \boldsymbol{q}_{chw,2} + \cdots + \boldsymbol{q}_{chw,\boldsymbol{n}} \tag{9}$$

$$\boldsymbol{T}_{cwout} \cdot \boldsymbol{q}_{cw} = \boldsymbol{T}_{cwout,1} \cdot \boldsymbol{q}_{cw,1} + \boldsymbol{T}_{cwout,2} \cdot \boldsymbol{q}_{cw,2} + \cdots + \boldsymbol{T}_{cwout,n} \cdot \boldsymbol{q}_{cw,n} \tag{10}$$

$$\boldsymbol{q}_{cw} = \boldsymbol{q}_{cw,1} + \boldsymbol{q}_{cw,2} + \cdots + \boldsymbol{q}_{cw,n} \tag{11}$$

### *3.5 Measurement uncertainty models (Likelihoods)*

According to the characteristics of measurement uncertainty mentioned in Section 2.2, the measured flow rates follow normal distributions as shown in Eq. (12), (13), (14) and (15) respectively. In these equations, only the measured water flow rate ($\tilde{\boldsymbol{q}}$) is available. The true water flow rate ($\boldsymbol{q}$), mean ($\mu$, systematic uncertainty) and standard deviation ($\sigma$, random

uncertainty) corresponding to each flow meter are unknown and should be quantified. These measurement uncertainty models are in fact the likelihoods in Bayes' theorem.

$$\tilde{\boldsymbol{q}}_{chw,i} \sim \boldsymbol{N}\left(\boldsymbol{q}_{chw,i} + \mu_{chwq,i},\ \sigma^2_{chwq,i}\right), \quad i = 1,2,...,n \tag{12}$$

$$\tilde{\boldsymbol{q}}_{cw,i} \sim \boldsymbol{N}\left(\boldsymbol{q}_{cw,i} + \mu_{cwq,i},\ \sigma^2_{cwq,i}\right), \quad i = 1,2,...,n \tag{13}$$

$$\tilde{\boldsymbol{q}}_{chw} \sim \boldsymbol{N}\left(\boldsymbol{q}_{chw} + \mu_{chwq},\ \sigma^2_{chwq}\right) \tag{14}$$

$$\tilde{\boldsymbol{q}}_{cw} \sim \boldsymbol{N}\left(\boldsymbol{q}_{cw} + \mu_{cwq},\ \sigma^2_{cwq}\right) \tag{15}$$

In MCMC sampling process, these unknown parameters involved should satisfy the distribution functions above and are constrained by the energy balance models described in Section 3.4. When the pre-set/enough iterations are done, these effective samples will be used to construct the posterior distributions of the unknown parameters involved and then further analysis can be conducted.

## 4. Description of test arrangement

The strategy is tested using site data. In practical application, the true values of measurements cannot be known exactly, which means that the measurement uncertainty of a sensor cannot be known exactly either. Even though the measurement uncertainty of site data can be quantified by the proposed strategy, it is very difficult to judge whether the quantified results are correct or not. Hence, four simulation tests with different levels of measurement uncertainty are conducted to further test and validate the strategy systematically. Details about the site test case and simulation test cases are introduced in this section.

### *4.1 Description of the site test case*

#### *4.1.1 Chiller system involved in the site test case*

The chiller system is equipped in a super high-rise commercial building in Hong Kong. The system equips six identical chillers, and each chiller is interlocked with a constant-speed cooling water pump and a constant-speed primary chilled water pump. The rated cooling capacity of each chiller is 7 230 kW, and the rated flow rates of each cooling water pump and primary chilled water pump are 410.1 L/s and 345.0 L/s respectively. More details about the chiller system can be found in references [34, 35].

The chilled water flow rate and the cooling water flow rate of each chiller are measured on-site, but the main chilled water flow rate and the main cooling water flow rate are not measured in the system. Even so, the proposed strategy is also applicable to the case. The

measurement uncertainty models are represented by Eq. (12) and (13), subject to the constraint (i.e. the energy balance model) shown in Eq. (7). In this paper, test results from one of the chillers are selected to demonstrate the use and the performance of the strategy. The data used in this site test case was collected on 31 Aug 2020 with a time interval of 5 minutes, and the chiller concerned ran 24 hours per day. There are 288 data sets in total.

*4.1.2 Prior distributions of unknown parameters in the site test case*

There are 6 unknown parameters to be quantified in this site test case, including the systematic uncertainties and the standard deviations of the random uncertainties of chilled water and cooling water flow meters, as well as the means of true chilled water and cooling water flow rates. The prior distributions of these unknown parameters can be assigned according to the rules described in Section 3.3, with the details shown in Table 1.

Table 1 Prior distributions of unknown parameters in the site test case

| No. | Parameter | Prior distribution |
|---|---|---|
| 1 | Systematic uncertainty of chilled water flow meter | $N(0, 21^2)$ |
| 2 | Systematic uncertainty of cooling water flow meter | $N(0, 25^2)$ |
| 3 | Random uncertainty of chilled water flow meter | $\chi^2(3)$ |
| 4 | Random uncertainty of cooling water flow meter | $\chi^2(3)$ |
| 5 | Mean of true chilled water flow rate | $N(345, 6.3^2)$ |
| 6 | Mean of true cooling water flow rate | $N(410.1, 7.5^2)$ |

### *4.2 Description of the simulation test cases*

*4.2.1 Chiller system model used in the simulation test cases*

A multiple water-cooled chiller system is simulated. The system consists of three identical chillers, three identical chilled water pumps and three identical cooling water pumps. The mathematical model of the chiller is obtained by referring to reference [36]. The full load coefficient of performance ($COP_{FL}$) of the chillers with different cooling capacities ($CP$) is represented by Eq. (16). The ratio ($\alpha$) of the actual (part-load) COP of the chiller to its full load COP is determined by Eq. (17), which is a function of the part load ratio ($r_p$). The actual COP and the power consumption ($P$) of the chillers can be calculated using Eq. (18) and Eq. (19) respectively.

$$COP_{FL} = 2.886\times10^{-9}\cdot CP^2 + 0.293\times10^{-4}\cdot CP + 4.711 \tag{16}$$

$$\alpha = -0.569\cdot r_p^3 - 0.258\cdot r_p^2 + 1.520\cdot r_p + 0.321 \tag{17}$$

$$COP = \alpha\cdot COP_{FL} \tag{18}$$

$$P = \frac{Q}{COP} \tag{19}$$

The rated cooling capacity of each chiller in this study is 600 kW. The full load COP is 4.73. The cooling load in the test period ranges between 1 200 kW and 1 800 kW as shown in Fig. 7 (94 points in total), with all three chillers running during the test period. The cooling load is equally distributed to each of the three chillers in the test, and the rated flow rates of the chilled water pumps and cooling water pumps are 28.6 L/s and 34.7 L/s respectively. In addition, the measurement uncertainty models are represented by Eq. (12)-(15), subject to constraints shown in Eq. (7)-(11).

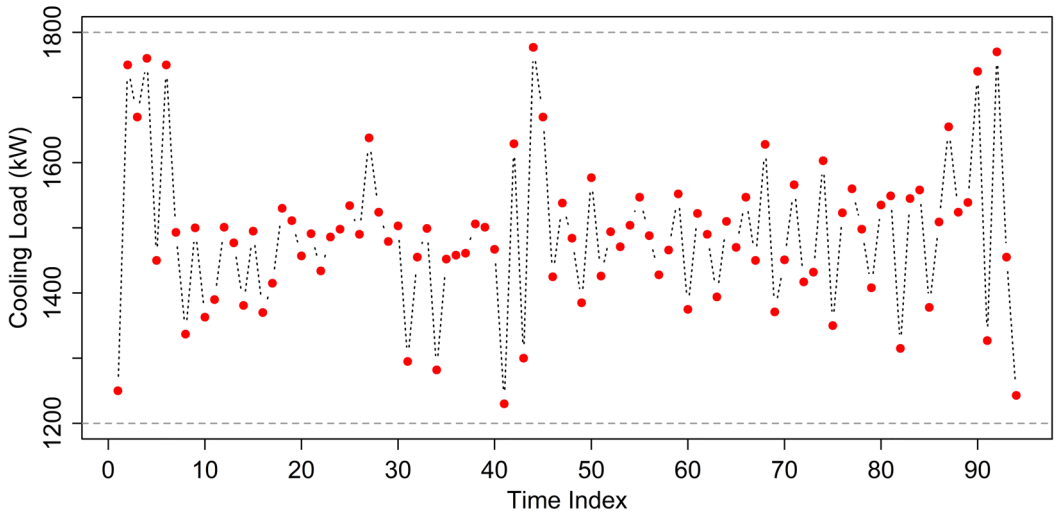


Fig. 7. Cooling load profile

*4.2.2 Prior distributions of unknown parameters in the simulation test cases*

There are eight flow meters in total in the chiller system used in the test, i.e., the chilled water and cooling water flow meters of each chiller and the main chilled water and cooling water flow meters. There are 22 unknown parameters in the test cases, including the systematic uncertainties and standard deviations of random uncertainties of each flow meter, and the means of true chilled water and cooling water flow rates of each chiller. The prior distributions of these unknown parameters are assigned according to the rules described in Section 3.3. The details are shown in Table 2.

Table 2 Prior distributions of unknown parameters in the simulation test cases

| No. | Parameter | Prior distribution |
|---|---|---|
| 1-3 | Systematic uncertainty of chilled water flow meter 1-3 | $N(0, 1.46^2)$ |
| 4-6 | Systematic uncertainty of cooling water flow meter 1-3 | $N(0, 1.79^2)$ |
| 7 | Systematic uncertainty of main chilled water flow meter | $N(0, 4.38^2)$ |
| 8 | Systematic uncertainty of main cooling water flow meter | $N(0, 5.37^2)$ |
| 9-11 | Random uncertainty of chilled water flow meter 1-3 | $\chi^2(3)$ |
| 12-14 | Random uncertainty of cooling water flow meter 1-3 | $\chi^2(3)$ |
| 15 | Random uncertainty of main chilled water flow meter | $\chi^2(3)$ |
| 16 | Random uncertainty of main cooling water flow meter | $\chi^2(3)$ |
| 17-19 | Mean of true chilled water flow rate from chiller 1-3 | $N(28.6, 0.438^2)$ |
| 20-22 | Mean of true cooling water flow rate from chiller 1-3 | $N(34.7, 0.531^2)$ |

*4.2.3 Measurement uncertainty generation*

In these test cases, chiller plant simulation is conducted without accounting for measurement errors. The "actual measurements" are generated by adding errors to the simulation test outputs. The simulation test outputs are considered to be the true values without measurement uncertainties. The measurement uncertainties of the flow meters are generated according to the characteristics of measurement uncertainty. As mentioned in Section 2.2, the measurement uncertainty of a sensor follows a normal distribution. Hence, the measurement uncertainty of each flow meter is generated randomly by a given normal distribution, as described in Eq. (20)-(23).

$$u_{chwq,i} \sim N(\mu_{chwq,i}, \sigma^2_{chwq,i}), \quad i = 1, 2, 3 \tag{20}$$

$$u_{cwq,i} \sim N(\mu_{cwq,i}, \sigma^2_{cwq,i}), \quad i = 1, 2, 3 \tag{21}$$

$$u_{chwq} \sim N(\mu_{chwq}, \sigma^2_{chwq}) \tag{22}$$

$$u_{cwq} \sim N(\mu_{cwq}, \sigma^2_{cwq}) \tag{23}$$

Because the sample size is limited and the generation of random numbers is pseudo-random, the generated measurement uncertainties may not follow the given normal distribution strictly. In addition, there is more than one variable should be considered simultaneously. Therefore, the conditioned Latin hypercube sampling (cLHS) method [37, 38] is used to solve this problem, as it can generate near-random samples for each variable from a multi-variable distribution. In this study, the measurement uncertainties of all flow meters are generated according to given normal distributions. 940 000 data sets are generated first, then 94 data sets are sampled from the population.

Table 3 lists the pre-set values of these unknown parameters in the simulation test cases, including the systematic uncertainties and the standard deviations of the random uncertainties of each flow meter. The levels of measurement uncertainties in the four simulation test cases are different. The systematic uncertainties of the flow meters in Case 1 and Case 4 are about 10% of the rated flow rates of corresponding water pumps, while in Case 2 and Case 3 they are about 5%. In addition, the systematic uncertainties of the flow meters in Case 1 and Case 2 are positive, which may result in that the measured flow rates are greater than the true flow rates. Conversely, the systematic uncertainties of the flow meters in Case 3 and Case 4 are negative, which may result in that the measured flow rates are less than the true flow rates. The standard deviations of the random uncertainties follow a slowly rising trend in all cases.

Table 3 Pre-set values of measurement uncertainties in the simulation test cases (Unit: L/s)

| Flow meter | Case 1 (10%) | Case 2 (5%) | Case 3 (-5%) | Case 4 (-10%) |
|---|---|---|---|---|
| *Systematic uncertainty* | | | | |
| Main chilled water flow meter | 8.50 | 4.50 | -4.50 | -8.50 |
| Chilled water flow meter 1 | 2.50 | 1.50 | -1.50 | -2.50 |
| Chilled water flow meter 2 | 2.75 | 1.75 | -1.75 | -2.75 |
| Chilled water flow meter 3 | 3.00 | 1.25 | -1.25 | -3.00 |
| Main cooling water flow meter | 10.00 | 5.00 | -5.00 | -10.00 |
| Cooling water flow meter 1 | 3.25 | 2.00 | -2.00 | -3.25 |
| Cooling water flow meter 2 | 3.75 | 1.50 | -1.50 | -3.75 |
| Cooling water flow meter 3 | 3.50 | 1.75 | -1.75 | -3.50 |
| *Standard deviation of random uncertainty* | | | | |
| Main chilled water flow meter | 1.50 | 1.75 | 2.00 | 2.25 |
| Chilled water flow meter 1 | 1.25 | 1.00 | 1.75 | 1.50 |
| Chilled water flow meter 2 | 0.75 | 1.50 | 1.25 | 2.00 |
| Chilled water flow meter 3 | 1.00 | 1.25 | 1.50 | 1.75 |
| Main cooling water flow meter | 1.75 | 2.00 | 2.25 | 2.50 |
| Cooling water flow meter 1 | 1.00 | 1.75 | 1.50 | 2.00 |
| Cooling water flow meter 2 | 1.25 | 1.50 | 2.00 | 1.75 |
| Cooling water flow meter 3 | 1.50 | 1.25 | 1.75 | 2.25 |

## 5. Measurement uncertainty quantification results and analysis

The proposed strategy is tested and validated by using it to quantify the measurement uncertainties of flow meters in five test cases, including a case using real site data and four simulation test cases with different levels of measurement uncertainties. The possible distributions (i.e. posterior distributions) of measurement uncertainties (both systematic and random uncertainties) are obtained. In order to systematically analyse and evaluate the results, 95% and/or 99% Bayesian credible intervals and the posterior means of the parameters to be

quantified are also presented. Moreover, in this study, the Site test case iterates 500 000 times per chain and each simulation test case iterate 2 000 times per chain for convergence. But the first $K$ samples ($K<N_{iter}$) are called "warmup" samples and should be discarded, the rest ($N_{iter}$ - $K$) are called "post-warmup" samples and are used to construct the posterior distributions. In this study, the number of warmup samples ($K$) is equal to half the number of iterations ($N_{iter}/2$).

### *5.1 Water flow measurement uncertainty quantification - Site test case*

The measurement uncertainties of both chilled water and cooling water flow meters can be quantified successfully. It does 500 000 iterations totally, but there are 250 000 "warmup" samples are discarded. In addition, a *thinning* technique is used to reduce the autocorrelations and chain length [29]. It saves every 250$^{th}$ sample from the Markov chain and the rest are discarded. Fig. 8 shows the traces and autocorrelations of the post-warmup MCMC samples in this test case. As can be seen from the figure, the Markov chains of random uncertainties are well convergent and their autocorrelations decay fast. Although the Markov chains of systematic uncertainties do not converge as well as the random uncertainties, they are also acceptable. These post-warmup MCMC samples can be used to construct the posterior distributions of the parameters involved.

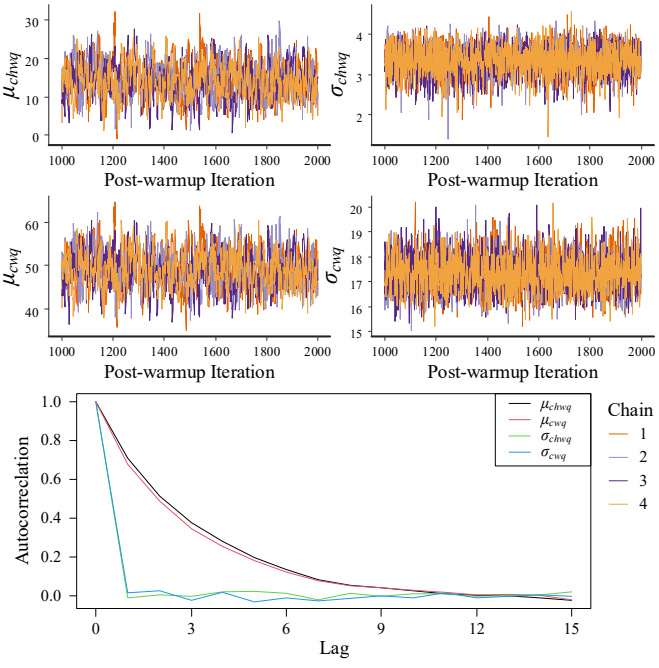


Fig. 8. Traces and autocorrelations of post-warmup MCMC samples in Site test case

Table 4 shows the quantified measurement uncertainties in the site test case. It can be observed that both the systematic uncertainty and the random uncertainty of the cooling water flow meter are larger than that of the chilled water flow meter. The posterior mean of the

systematic uncertainty of the chilled water flow meter is 4.17% of the rated flow rate of the chilled water pump, while the posterior mean of the systematic uncertainty of the cooling water flow meter is 11.99% of the rated flow rate of the cooling water pump.

Table 4 Quantified measurement uncertainties in the site test case

| Flow meter | 95% credible interval (L/s) | Posterior mean (L/s) | Percentage |
|---|---|---|---|
| *Systematic uncertainty* | | | |
| Chilled water flow meter | [5.53, 23.18] | 14.39 | 4.17% |
| Cooling water flow meter | [41.16, 57.30] | 49.18 | 11.99% |
| *Standard deviation of random uncertainty* | | | |
| Chilled water flow meter | [2.56, 4.00] | 3.34 | - |
| Cooling water flow meter | [16.00, 18.81] | 17.34 | - |

The ranges of the 95% credible intervals are relatively narrow. They are 17.65 L/s and 16.14 L/s for the systematic uncertainties of the chilled water and cooling water flow meters respectively. The corresponding random uncertainties are 1.44 L/s and 2.81 L/s for the chilled water and cooling water flow meters respectively, which are rather small. In statistics, a narrow credible interval can generally provide more information about the population parameter. Therefore, the above results seem to be reliable. According to the specifications of the flow meters used, the accuracy of the insertion flow meters is about 2% [9], and actual site installation and aging may also affect the accuracy of flow measurements. Hence, a systematic uncertainty of 4.17% is quite acceptable for chilled water flow meters in practical buildings. Concerning the cooling water flow meter, a systematic uncertainty of 11.99% is obviously beyond normal deviations caused by meter accuracy and installation, giving it a high probability of being in an unhealthy condition. These results may also reflect errors from other sensors, like the power meter and temperature sensors.

It is hard to fully confirm whether the quantified results are correct because the measurement errors and uncertainties of the two flow meters cannot be known exactly. On-site verification of the flow meters at such a range of flow measurement deviation is very difficult due to the limitations of site conditions. In fact, the true flow rate cannot be obtained no matter how accurate the instruments used are. Therefore, simulation tests are a simpler and more direct means of further testing and validating the strategy.

### *5.2 Water flow measurement uncertainty quantification - Simulation test case 1 (systematic uncertainty: 10%)*

Fig. 9 and Fig. 10 show the traces and autocorrelations of post-warmup MCMC samples in this test case respectively. There are 1 000 “warmup” samples are discarded. As can be seen from the figures, the Markov chains of each parameter are well converged and the autocorrelations of MCMC samples are reduced rapidly. These post-warmup MCMC samples can be used to construct the posterior distributions of the parameters involved.

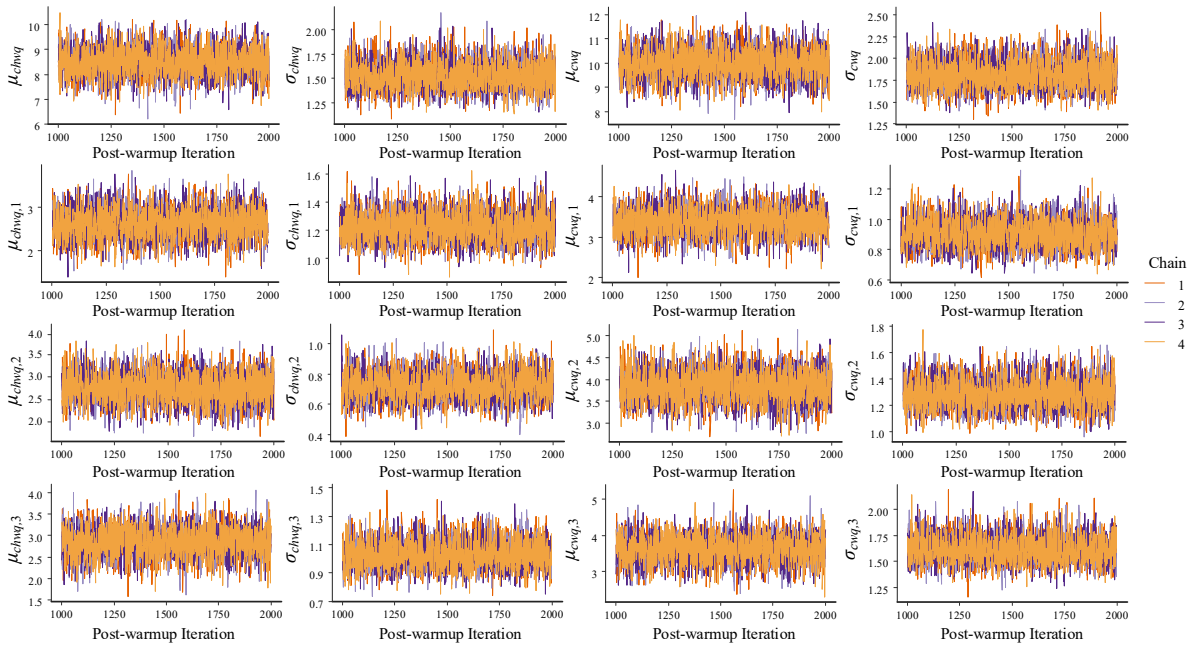


Fig. 9. Traces of post-warmup MCMC samples in Simulation test case 1

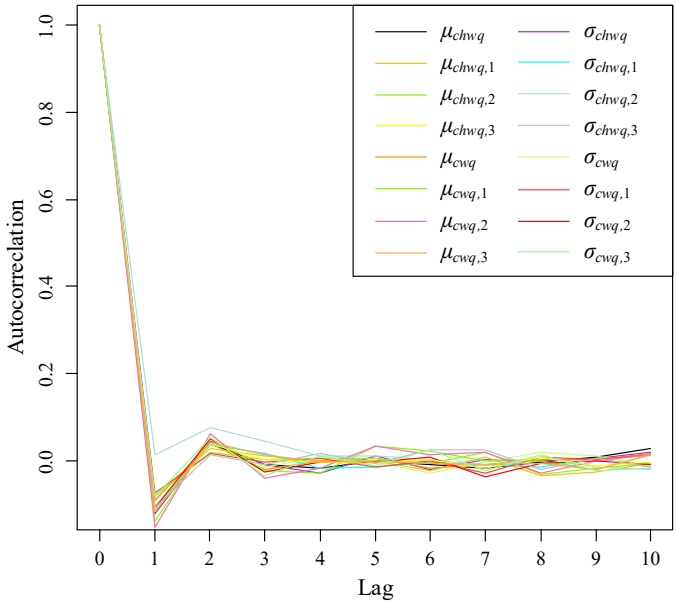


Fig. 10. Autocorrelations of post-warmup MCMC samples in Simulation test case 1

Table 5 shows the quantified measurement uncertainties in Simulation test case 1, where the systematic uncertainties of the water flow meters are set to around 10% of the rated flow rates of the corresponding pumps. The 95% credible intervals and the posterior means are

presented. The pre-set values of the measurement uncertainties (both the systematic uncertainties and the standard deviations of random uncertainties) of the flow meters are also listed in the table for comparison. As shown in Table 5, the pre-set values fall within the 95% credible intervals, and the posterior means are very close to the pre-set values. Particularly for the systematic uncertainties of the main chilled water and cooling water flow meters, their posterior means are almost the same as their pre-set values.

Table 5 Quantified measurement uncertainties in Simulation test case 1

| Flow meter | Pre-set value (L/s) | 95% credible interval (L/s) | Posterior mean (L/s) | Relative error (%) | Relative systematic uncertainty (%) |
|---|---|---|---|---|---|
| *Systematic uncertainty* | | | | | |
| Main chilled water flow meter | 8.50 | [7.40, 9.68] | 8.52 | 0.24 | 0.02 |
| Chilled water flow meter 1 | 2.50 | [1.95, 3.32] | 2.63 | 5.20 | 0.45 |
| Chilled water flow meter 2 | 2.75 | [2.11, 3.41] | 2.77 | 0.73 | 0.07 |
| Chilled water flow meter 3 | 3.00 | [2.15, 3.48] | 2.84 | 5.30 | 0.56 |
| Main cooling water flow meter | 10.00 | [8.77, 11.17] | 9.99 | 0.10 | 0.01 |
| Cooling water flow meter 1 | 3.25 | [2.73, 4.06] | 3.38 | 4.00 | 0.37 |
| Cooling water flow meter 2 | 3.75 | [3.15, 4.54] | 3.85 | 2.67 | 0.29 |
| Cooling water flow meter 3 | 3.50 | [2.86, 4.32] | 3.62 | 3.43 | 0.35 |
| *Standard deviation of random uncertainty* | | | | | |
| Main chilled water flow meter | 1.50 | [1.27, 1.83] | 1.53 | 2.00 | - |
| Chilled water flow meter 1 | 1.25 | [1.03, 1.44] | 1.22 | 2.40 | - |
| Chilled water flow meter 2 | 0.75 | [0.55, 0.91] | 0.72 | 4.00 | - |
| Chilled water flow meter 3 | 1.00 | [0.85, 1.23] | 1.03 | 3.00 | - |
| Main cooling water flow meter | 1.75 | [1.53, 2.16] | 1.80 | 2.86 | - |
| Cooling water flow meter 1 | 1.00 | [0.73, 1.10] | 0.90 | 10.00 | - |
| Cooling water flow meter 2 | 1.25 | [1.08, 1.52] | 1.28 | 2.40 | - |
| Cooling water flow meter 3 | 1.50 | [1.38, 1.89] | 1.62 | 8.00 | - |

The “relative error” and the “relative systematic uncertainty” are also presented in Table 5. Where, the posterior mean of a parameter is regarded as its estimated value. The relative error is defined as the absolute error of uncertainty estimation (i.e. the difference between the pre-set value of the uncertainty and the posterior mean) divided by the pre-set value of the uncertainty. Similarly, the relative systematic uncertainty is defined as the absolute error divided by the design flow rate associated with the flow meter concerned or the rated flow rate of the corresponding water pump. It can be observed that the maximum relative errors are 5.30% and 10.00% for the quantified systematic uncertainties and quantified random uncertainties respectively, indicating reasonably good accuracy. In addition, the relative

systematic uncertainties are very small, ranging between 0.01% and 0.56%. This strategy can therefore be used to validate flow meters and improve measurement accuracy effectively. In fact, relative systematic uncertainty may be a better index to evaluate the quantified results in practical application, since the true systematic uncertainties (pre-set values) are unknown. It can be seen that the measurement uncertainties of flow meters can be quantified successfully with high accuracy in this test case.

### *5.3 Water flow measurement uncertainty quantification - Simulation test case 2 (systematic uncertainty: 5%)*

Fig. 11 and Fig. 12 show the traces and autocorrelations of post-warmup MCMC samples in this test case respectively. It can be observed that the Markov chains of each parameter are well converged and the autocorrelations of MCMC samples are reduced rapidly. These post-warmup MCMC samples can be used to construct the posterior distributions of the parameters involved.

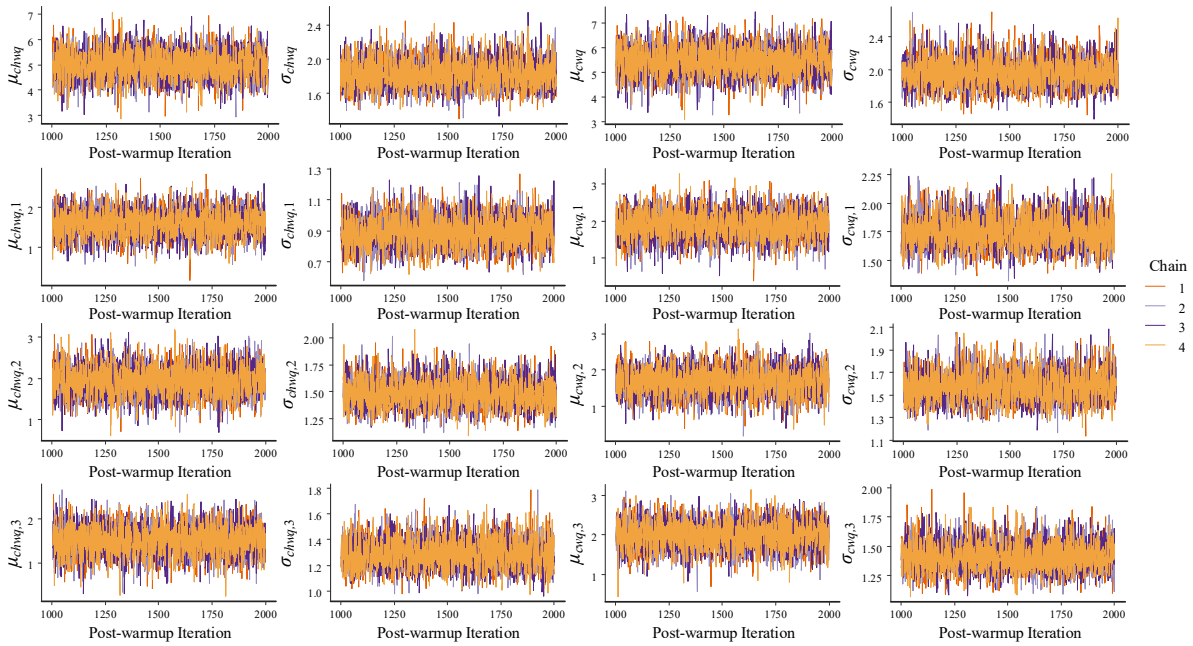


Fig. 11. Traces of post-warmup MCMC samples in Simulation test case 2

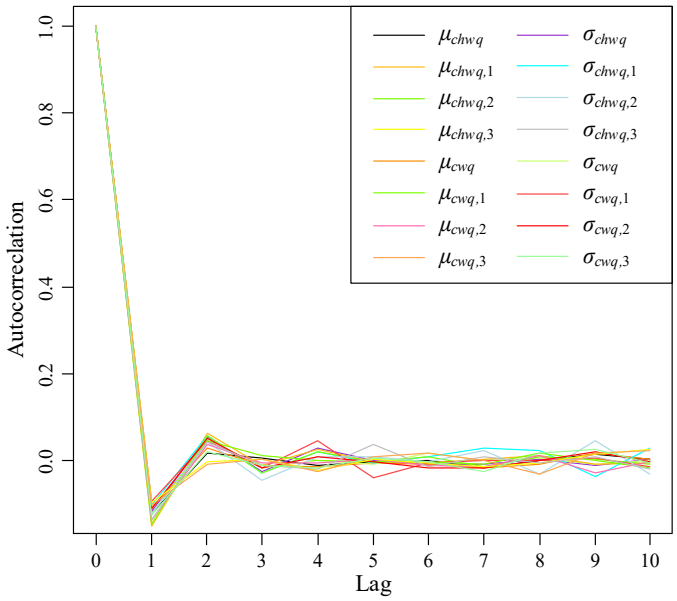


Fig. 12. Autocorrelations of post-warmup MCMC samples in Simulation test case 2

Table 6 shows the quantified measurement uncertainties in Simulation test case 2, where the systematic uncertainties of the water flow meters are set to around 5% of the rated flow rates of the corresponding pumps. It can be observed that the pre-set values fall within the 95% credible intervals, and since the posterior means are close to the pre-set values, the measurement uncertainties in this test case have been quantified successfully. For the quantified systematic uncertainties in this test case, the relative errors are larger than that in Simulation test case 1, as the maximum relative error is 20.00%. The relative systematic uncertainties are still small (0.31-0.87%). The strategy can still be used to validate flow meters and improve measurement accuracy. For the quantified random uncertainties in this test case, the relative errors are small, with a maximum value of 12.80%. Therefore, the strategy performs better in quantifying random uncertainties than systematic uncertainties in this test case.

Table 6 Quantified measurement uncertainties in Simulation test case 2

| Flow meter | Pre-set value (L/s) | 95% credible interval (L/s) | Posterior mean (L/s) | Relative error (%) | Relative systematic uncertainty (%) |
|---|---|---|---|---|---|
| *Systematic uncertainty* | | | | | |
| Main chilled water flow meter | 4.50 | [3.89, 6.11] | 5.02 | 11.55 | 0.61 |
| Chilled water flow meter 1 | 1.50 | [0.90, 2.26] | 1.59 | 6.00 | 0.31 |
| Chilled water flow meter 2 | 1.75 | [1.25, 2.66] | 1.94 | 10.86 | 0.66 |
| Chilled water flow meter 3 | 1.25 | [0.84, 2.16] | 1.50 | 20.00 | 0.87 |
| Main cooling water flow meter | 5.00 | [4.29, 6.63] | 5.48 | 9.60 | 0.46 |
| Cooling water flow meter 1 | 2.00 | [1.14, 2.60] | 1.89 | 5.50 | 0.32 |
| Cooling water flow meter 2 | 1.50 | [0.94, 2.41] | 1.68 | 12.00 | 0.52 |
| Cooling water flow meter 3 | 1.75 | [1.29, 2.67] | 1.98 | 13.14 | 0.66 |
| *Standard deviation of random uncertainty* | | | | | |
| Main chilled water flow meter | 1.75 | [1.52, 2.18] | 1.83 | 4.57 | - |
| Chilled water flow meter 1 | 1.00 | [0.70, 1.09] | 0.89 | 11.00 | - |
| Chilled water flow meter 2 | 1.50 | [1.25, 1.76] | 1.48 | 1.33 | - |
| Chilled water flow meter 3 | 1.25 | [1.08, 1.52] | 1.29 | 3.20 | - |
| Main cooling water flow meter | 2.00 | [1.64, 2.33] | 1.96 | 2.00 | - |
| Cooling water flow meter 1 | 1.75 | [1.49, 2.04] | 1.75 | 0.00 | - |
| Cooling water flow meter 2 | 1.50 | [1.34, 1.84] | 1.58 | 5.33 | - |
| Cooling water flow meter 3 | 1.25 | [1.19, 1.67] | 1.41 | 12.80 | - |

### *5.4 Water flow measurement uncertainty quantification - Simulation test case 3 (systematic uncertainty: -5%)*

Fig. 13 and Fig. 14 show the traces and autocorrelations of post-warmup MCMC samples in this test case respectively. It can be observed that the Markov chains of each parameter are well converged and the autocorrelations of MCMC samples are reduced rapidly. These post-warmup MCMC samples can be used to construct the posterior distributions of the parameters involved.

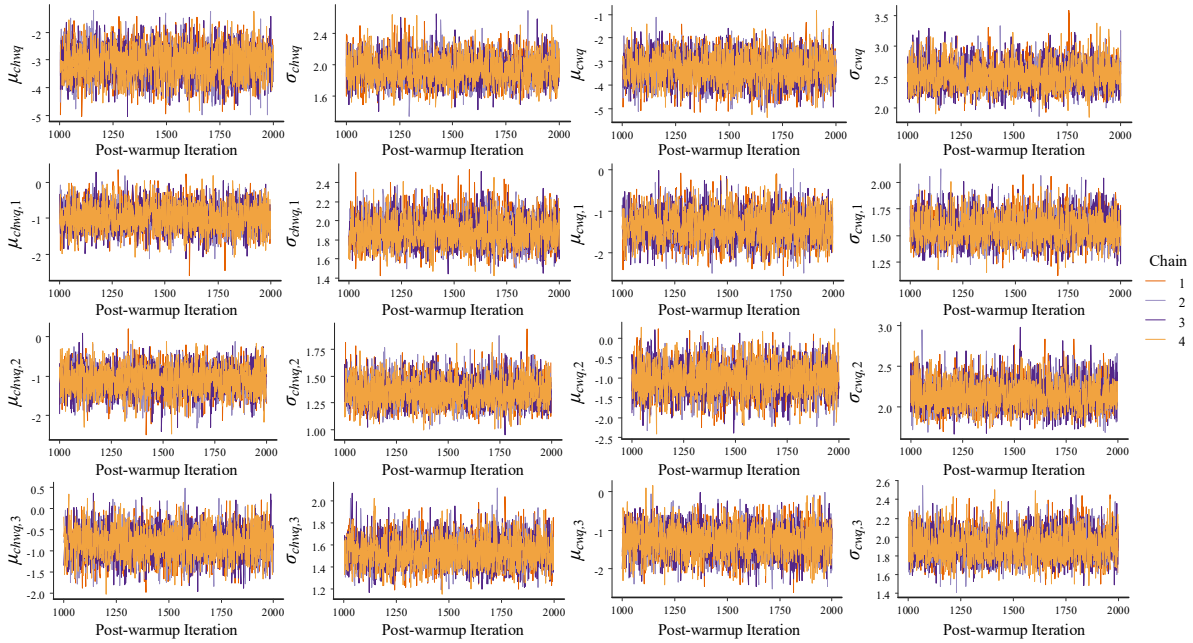


Fig. 13. Traces of post-warmup MCMC samples in Simulation test case 3

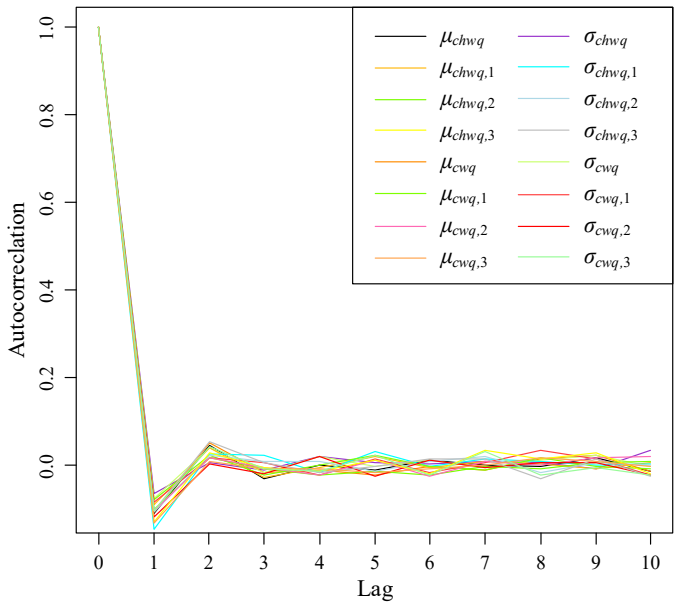


Fig. 14. Autocorrelations of post-warmup MCMC samples in Simulation test case 3

Table 7 shows the quantified measurement uncertainties in Simulation test case 3, where the systematic uncertainties of the water flow meters are set to be around -5% of the rated flow rate of corresponding pumps. For the quantified systematic uncertainties of the main chilled water and cooling water flow meters, the pre-set values do not fall within the 95% credible intervals, and so the 99% credible intervals are also presented. It can be observed that the pre-set values are very close to the lower limits of the 99% credible intervals. The differences between the pre-set values and the posterior means are significant. For the quantified systematic uncertainties of the other flow meters in this test case, the pre-set values are close

to the lower limits of the 95% credible intervals, and the differences between the pre-set values and the posterior means are also very significant. The relative errors in this test case are more significant than that in Simulation test case 1 and Simulation test case 2, with the maximum error being 38.57%. The relative systematic uncertainties are still within a relatively small range (1.33-2.24%). The results show that the strategy is still effective for validating flow meters and improving measurement accuracy, and can also provide valuable and meaningful information in practical application. For the quantified random uncertainties of the flow meters in this test case, the pre-set values fall within the 95% credible intervals, and the posterior means are very close to the pre-set values. The maximum relative error is 12.44% and the relative errors are within an acceptable range. The random uncertainties of flow meters in this test case are quantified with satisfactory accuracy. The strategy performs better in quantifying random uncertainties compared with systematic uncertainties in this test case.

Table 7 Quantified measurement uncertainties in Simulation test case 3

| Flow meter | Pre-set value (L/s) | 95% credible interval (L/s) | 99% credible interval* (L/s) | Posterior mean (L/s) | Relative error (%) | Relative systematic uncertainty (%) |
|---|---|---|---|---|---|---|
| *Systematic uncertainty* | | | | | | |
| Main chilled water flow meter | -4.50 | [-4.27, -1.97] | [-4.60, -1.61] | -3.11 | 30.89 | 1.62 |
| Chilled water flow meter 1 | -1.50 | [-1.71, -0.25] | - | -0.98 | 34.67 | 1.82 |
| Chilled water flow meter 2 | -1.75 | [-1.78, -0.45] | - | -1.11 | 36.57 | 2.24 |
| Chilled water flow meter 3 | -1.25 | [-1.56, -0.11] | - | -0.83 | 33.60 | 1.47 |
| Main cooling water flow meter | -5.00 | [-4.54, -2.09] | [-4.94, -1.74] | -3.31 | 33.80 | 1.62 |
| Cooling water flow meter 1 | -2.00 | [-2.08, -0.63] | - | -1.34 | 33.00 | 1.90 |
| Cooling water flow meter 2 | -1.50 | [-1.83, -0.26] | - | -1.04 | 30.67 | 1.33 |
| Cooling water flow meter 3 | -1.75 | [-2.06, -0.54] | - | -1.28 | 26.86 | 1.35 |
| *Standard deviation of random uncertainty* | | | | | | |
| Main chilled water flow meter | 2.00 | [1.61, 2.30] | - | 1.93 | 3.50 | - |
| Chilled water flow meter 1 | 1.75 | [1.62, 2.22] | - | 1.89 | 8.00 | - |
| Chilled water flow meter 2 | 1.25 | [1.13, 1.62] | - | 1.35 | 8.00 | - |
| Chilled water flow meter 3 | 1.50 | [1.30, 1.82] | - | 1.54 | 2.67 | - |
| Main cooling water flow meter | 2.25 | [2.14, 2.98] | - | 2.53 | 12.44 | - |
| Cooling water flow meter 1 | 1.50 | [1.32, 1.86] | - | 1.57 | 4.67 | - |
| Cooling water flow meter 2 | 2.00 | [1.83, 2.52] | - | 2.14 | 7.00 | - |
| Cooling water flow meter 3 | 1.75 | [1.63, 2.23] | - | 1.91 | 9.14 | - |

*Only the 99% credible intervals of the parameters whose pre-set values do not fall within their 95% credible intervals are presented.

### *5.5 Water flow measurement uncertainty quantification - Simulation test case 4 (systematic uncertainty: -10%)*

Fig. 15 and Fig. 16 show the traces and autocorrelations of post-warmup MCMC samples in this test case respectively. It can be observed that the Markov chains of each parameter are well converged and the autocorrelations of MCMC samples are reduced rapidly. These post-warmup MCMC samples can be used to construct the posterior distributions of the parameters involved.

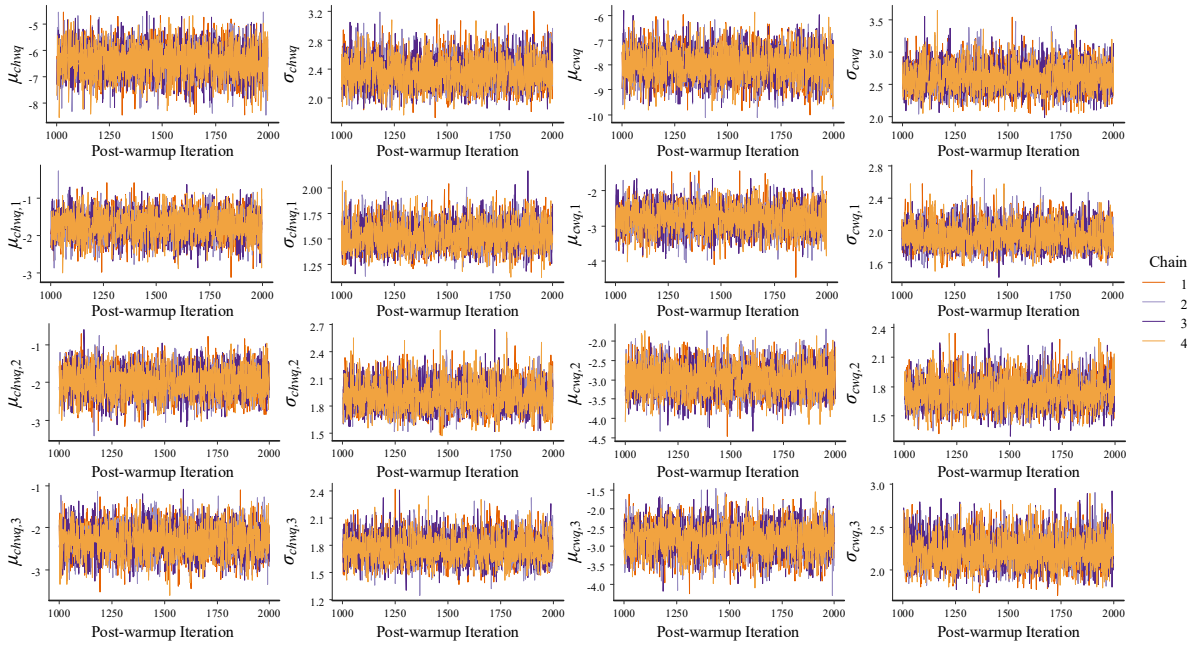


Fig. 15. Traces of post-warmup MCMC samples in Simulation test case 4

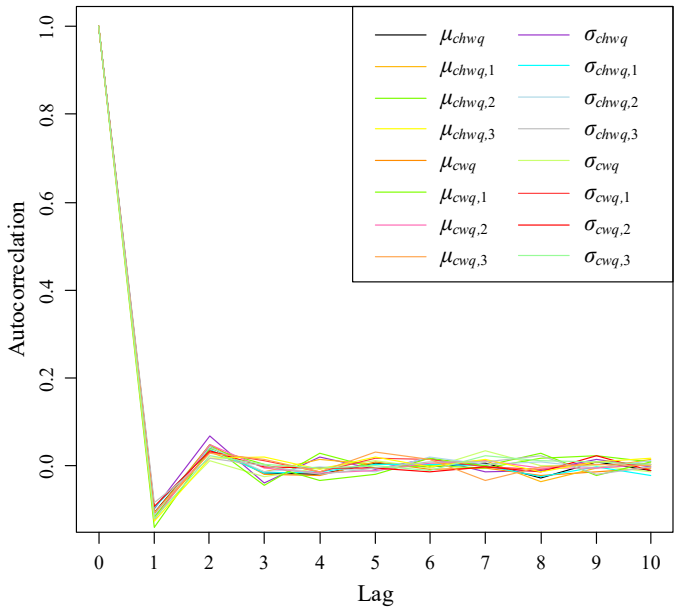


Fig. 16. Autocorrelations of post-warmup MCMC samples in Simulation test case 4

Table 8 shows the quantified measurement uncertainties in Simulation test case 4, where the systematic uncertainties of the water flow meters are set to around -10% of the rated flow rate of the corresponding pumps. Both the 95% and 99% credible intervals of the quantified systematic uncertainties in this test case are presented. Besides the main chilled water and cooling water flow meters, the pre-set values of the quantified systematic uncertainties fall within the 99% credible intervals. The differences between the pre-set values and the posterior means are significant, leading to large relative errors with a maximum value of 30.40%. The relative systematic uncertainties range between 1.27% and 2.66%. Similar to the previous cases, the strategy can provide valuable and meaningful information in application. For the quantified random uncertainties in this test case, the pre-set values fall within the 95% credible intervals, and the posterior means are very close to the pre-set values. The maximum relative error is 4.50% and the relative errors are within an acceptable range. The strategy also performs better in quantifying random uncertainties than systematic uncertainties in this test case.

Table 8 Quantified measurement uncertainties in Simulation test case 4

| Flow meter | Pre-set value (L/s) | 95% credible interval (L/s) | 99% credible interval (L/s) | Posterior mean (L/s) | Relative error (%) | Relative systematic uncertainty (%) |
|---|---|---|---|---|---|---|
| *Systematic uncertainty* | | | | | | |
| Main chilled water flow meter | -8.50 | [-7.64, -5.25] | [-8.16, -4.80] | -6.44 | 24.24 | 2.40 |
| Chilled water flow meter 1 | -2.50 | [-2.44, -1.06] | [-2.68, -0.85] | -1.74 | 30.40 | 2.66 |
| Chilled water flow meter 2 | -2.75 | [-2.74, -1.26] | [-2.98, -1.06] | -1.99 | 27.64 | 2.66 |
| Chilled water flow meter 3 | -3.00 | [-3.03, -1.57] | [-3.25, -1.40] | -2.30 | 23.33 | 2.45 |
| Main cooling water flow meter | -10.00 | [-9.23, -6.74] | [-9.60, -6.34] | -7.98 | 20.20 | 1.94 |
| Cooling water flow meter 1 | -3.25 | [-3.56, -2.08] | [-3.80, -1.85] | -2.81 | 13.54 | 1.27 |
| Cooling water flow meter 2 | -3.75 | [-3.73, -2.23] | [-3.95, -2.01] | -2.99 | 20.27 | 2.19 |
| Cooling water flow meter 3 | -3.50 | [-3.62, -2.04] | [-3.86, -1.75] | -2.82 | 19.43 | 1.96 |
| *Standard deviation of random uncertainty* | | | | | | |
| Main chilled water flow meter | 2.25 | [1.98, 2.79] | - | 2.35 | 4.44 | - |
| Chilled water flow meter 1 | 1.50 | [1.29, 1.82] | - | 1.54 | 2.67 | - |
| Chilled water flow meter 2 | 2.00 | [1.63, 2.25] | - | 1.91 | 4.50 | - |
| Chilled water flow meter 3 | 1.75 | [1.49, 2.07] | - | 1.77 | 1.14 | - |
| Main cooling water flow meter | 2.50 | [2.23, 3.07] | - | 2.60 | 4.00 | - |
| Cooling water flow meter 1 | 2.00 | [1.66, 2.28] | - | 1.94 | 3.00 | - |
| Cooling water flow meter 2 | 1.75 | [1.46, 2.06] | - | 1.73 | 1.14 | - |
| Cooling water flow meter 3 | 2.25 | [1.90, 2.61] | - | 2.22 | 1.33 | - |

### *5.6 Comparison between the results of the four simulation test cases*

According to the outputs of the four simulation test cases presented in Section 5.2-5.5, the measurement uncertainties of water flow meters, including both the systematic uncertainties and the random uncertainties, can be quantified effectively by the proposed strategy. Fig. 17 summarizes the measurement uncertainty quantification results of the four simulation test cases. The relative errors and absolute errors of the measurement uncertainty quantification are presented. It can be observed that the errors of quantifying the random uncertainties of flow meters in all cases are very small, but the errors of quantifying the systematic uncertainties of flow meters vary from case to case. The errors are small for Case 1 and Case 2, but they are significant for Case 3 and Case 4.

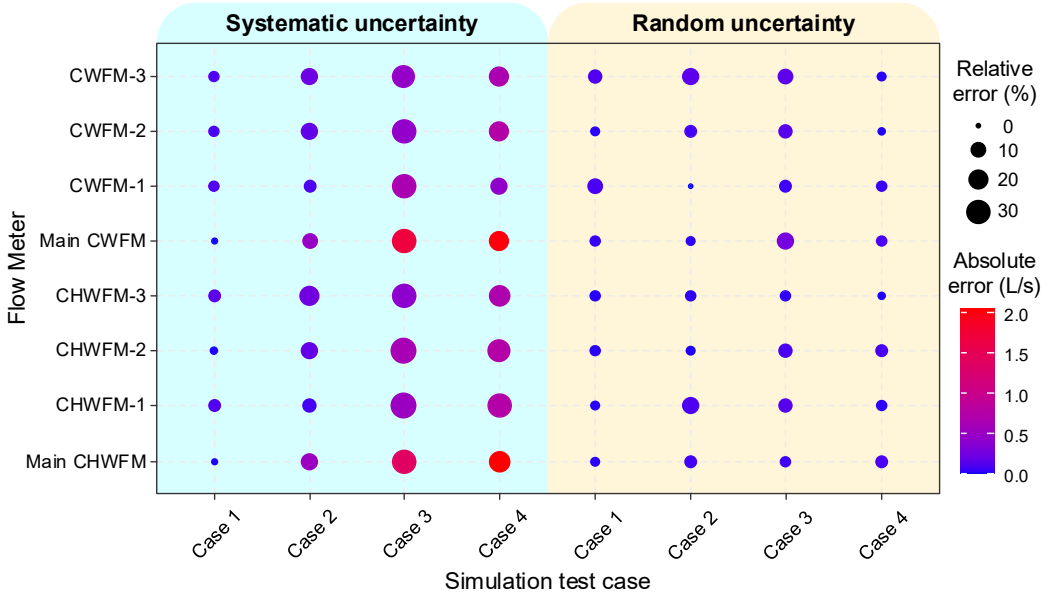


Fig. 17. Relative errors and absolute errors of measurement uncertainty quantification for simulation test cases

The proposed strategy performs very well in quantifying systematic uncertainties in Simulation test case 1 and 2. Although the performance of the strategy in quantifying systematic uncertainties in Simulation test case 3 and 4 is not as good as that in Simulation test case 1 and 2, its performance is still acceptable. The strategy is still effective for validating flow meters and improving measurement accuracy and can provide valuable and meaningful information in practical application. In addition, the random uncertainties of the flow meters can be quantified accurately by the strategy no matter how significant they are. In general, the strategy performs better in quantifying random uncertainties than systematic uncertainties.

The levels of the quantified measurement uncertainties in the four simulation test cases are consistent with the levels of the pre-set measurement uncertainties. In other words, the

levels of the measurement uncertainties of different flow meters can be identified by the strategy. The information is also meaningful and valuable in practical application. If the identified measurement uncertainties of one or more flow meters are obviously higher than that of other flow meters, more attention should be paid to these flow meters and calibrations on the measurement accuracy of these flow meters are needed or decisions requiring flow rate measurements of high accuracy should be avoided. For example, as presented in Section 5.1, the quantified measurement uncertainty of the cooling water flow meter in the site test case is much larger than the typical uncertainty range of flow measurement. If this cooling water flow measurement is used by a critical decision-making strategy, priority should be given to check/calibrate the flow meter or re-consider the decision-making strategy itself.

As mentioned in Section 3.2, both prior distributions and likelihoods may affect posterior distributions. It is possible to improve the accuracy of the proposed strategy from these two aspects. The likelihoods are associated with observational data. In principle, the posterior distributions are mainly affected by likelihoods if the quantity of observational data is large enough. However, the computational load will increase significantly if the quantity of observational data increases. Therefore, the size of the observational data cannot be increased without limit. A trade-off between the quantity of observational data and the computational load should be made. On the other hand, the assignments of the prior distributions of the parameters to be quantified are based on expert judgement. A good prior distribution will be of great help in accurately quantifying the measurement uncertainty. Maximum utilization of information about the parameters to be quantified should be achieved to obtain the best prior distributions.

The proposed measurement uncertainty quantification strategy is promising to be put into practice. The flow meters can be calibrated at any time by the strategy. A threshold of acceptable uncertainty can be set for each flow meter. If the quantified uncertainty of a flow meter is greater than the threshold, the operators can conduct an on-site calibration for the flow meter or replace the flow meter directly, and the impacts of the unacceptable uncertainty on system operation can be reduced.

## 6. Conclusions

This study proposed a flow measurement uncertainty quantification strategy which directly quantifies measurement uncertainties of water flow meters using a Bayesian approach. Bayesian inference and Markov chain Monte Carlo sampling methods are used. Both the

systematic uncertainties and the random uncertainties of flow meters in chiller systems are considered, and the energy balance models are taken as the constraints to MCMC sampling. The site data collected from a chiller system are used to test the strategy, and four simulation test cases with different levels of measurement uncertainties are conducted to systematically test and validate the strategy. Based on the results of these test cases, detailed conclusions can be drawn as follows.

- The proposed strategy can effectively quantify the measurement uncertainties (both systematic and random uncertainties) of chilled water and cooling water flow meters in chiller systems.
- The performance of the strategy in quantifying systematic uncertainties is satisfactory. The strategy is effective for validating flow meters and improving their measurement accuracy, and it can provide valuable and meaningful information in practical application.
- The random uncertainties can be quantified accurately by the proposed strategy no matter how significant they are. The strategy performs better in quantifying random uncertainties than systematic uncertainties.
- The levels of measurement uncertainties of different flow meters can be identified by the proposed strategy. It can be used to detect which flow meters need to be calibrated and assess the reliability of flow measurement, particularly concerning critical decision-making.

In practical application, factors such as data quality and volume, may affect the performance of the proposed strategy. Further research on data pre-processing is needed. In addition, the assignment of prior distributions is also worthy of further study.

## Acknowledgements

The research presented in this paper is financially supported by a General Research Fund (152053/21E) of the Research Grant Council (RGC) of the Hong Kong SAR.

## References

[1] Song K, Jang Y, Park M, Lee HS, Ahn J. Energy efficiency of end-user groups for personalized HVAC control in multi-zone buildings. Energy. 2020;206.

[2] Sun SB, Li GN, Chen HX, Huang QY, Shi SB, Hu WJ. A hybrid ICA-BPNN-based FDD strategy for refrigerant charge faults in variable refrigerant flow system. Applied Thermal Engineering. 2017;127:718-28.

[3] Karami M, Wang LP. Particle Swarm optimization for control operation of an all-variable speed water-cooled chiller plant. Applied Thermal Engineering. 2018;130:962-78.

[4] Mu BJ, Li YY, House JM, Salsbury TI. Real-time optimization of a chilled water plant with parallel chillers based on extremum seeking control. Applied Energy. 2017;208:766-81.

[5] Teimourzadeh H, Jabari F, Mohammadi-Ivatloo B. An augmented group search optimization algorithm for optimal cooling-load dispatch in multi-chiller plants. Computers & Electrical Engineering. 2020;85.

[6] Yan B, Li XW, Malkawi AM, Augenbroe G. Quantifying uncertainty in outdoor air flow control and its impacts on building performance simulation and fault detection. Energy and Buildings. 2017;134:115-28.

[7] Goyal S, Ingley HA, Barooah P. Effect of various uncertainties on the performance of occupancy-based optimal control of HVAC zones. 2012 IEEE 51st IEEE conference on decision and control (CDC): IEEE; 2012. p. 7565-70.

[8] Liao YD, Huang GS, Sun YJ, Zhang LF. Uncertainty analysis for chiller sequencing control. Energy and Buildings. 2014;85:187-98.

[9] ASHRAE. Guideline 14-2014: Measurement of energy, demand, and water savings. 2014.

[10] Zhuang CQ, Wang SW, Shan K. A risk-based robust optimal chiller sequencing control strategy for energy-efficient operation considering measurement uncertainties. Applied Energy. 2020;280.

[11] Zhuang CQ, Wang SW. Risk-based online robust optimal control of air-conditioning systems for buildings requiring strict humidity control considering measurement uncertainties. Applied Energy. 2020;261.

[12] Huang GS, Sun YJ, Li P. Fusion of redundant measurements for enhancing the reliability of total cooling load based chiller sequencing control. Automation in Construction. 2011;20:789-98.

[13] Sun YJ, Wang SW, Huang GS. Chiller sequencing control with enhanced robustness for energy efficient operation. Energy and Buildings. 2009;41:1246-55.

[14] Shi WT, Jin XQ, Wang YJ. Evaluation of energy saving potential of HVAC system by operation data with uncertainties. Energy and Buildings. 2019;204.

[15] Yang XB, Jin XQ, Du ZM, Fan B, Zhu YH. Optimum operating performance based online fault-tolerant control strategy for sensor faults in air conditioning systems. Automation in Construction. 2014;37:145-54.

[16] Guide 98-3, Uncertainty of measurement-Part 3: Guide to the expression of uncertainty in measurement (GUM: 1995): ISO/IEC; 2008.

[17] Tian W, Heo Y, de Wilde P, Li ZY, Yan D, Park CS, et al. A review of uncertainty analysis in building energy assessment. Renewable & Sustainable Energy Reviews. 2018;93:285-301.

[18] Kennedy MC, O'Hagan A. Bayesian calibration of computer models. Journal of the Royal Statistical Society Series B-Statistical Methodology. 2001;63:425-50.

[19] Heo Y, Choudhary R, Augenbroe GA. Calibration of building energy models for retrofit analysis under uncertainty. Energy and Buildings. 2012;47:550-60.

[20] Chong A, Lam KP, Pozzi M, Yang JZJ. Bayesian calibration of building energy models with large datasets. Energy and Buildings. 2017;154:343-55.

[21] Booth AT, Choudhary R, Spiegelhalter DJ. Handling uncertainty in housing stock models. Building and Environment. 2012;48:35-47.

[22] Liu Y, Dinh NT, Smith RC, Sun XD. Uncertainty quantification of two-phase flow and boiling heat transfer simulations through a data-driven modular Bayesian approach. International Journal of Heat and Mass Transfer. 2019;138:1096-116.

[23] Liu Y, Wang DW, Sun XD, Liu Y, Dinh N, Hu R. Uncertainty quantification for Multiphase-CFD simulations of bubbly flows: a machine learning-based Bayesian approach supported by high-resolution experiments. Reliability Engineering & System Safety. 2021;212.

[24] Zhu CQ, Tian W, Yin BQ, Li ZY, Shi JX. Uncertainty calibration of building energy models by combining approximate Bayesian computation and machine learning algorithms. Applied Energy. 2020;268.

[25] Burkhart MC, Heo Y, Zavala VM. Measurement and verification of building systems under uncertain data: A Gaussian process modeling approach. Energy and Buildings. 2014;75:189-98.

[26] Heo Y, Zavala VM. Gaussian process modeling for measurement and verification of building energy savings. Energy and Buildings. 2012;53:7-18.

[27] Yu FW, Chan KT. Optimum load sharing strategy for multiple-chiller systems serving air-conditioned buildings. Building and Environment. 2007;42:1581-93.

[28] Vehtari A, Gelman A, Simpson D, Carpenter B, Bürkner P-C. Rank-normalization, folding, and localization: An improved $\hat{R}$ for assessing convergence of MCMC. Bayesian Analysis. 2021;1:1-28.

[29] Annis J, Miller BJ, Palmeri TJ. Bayesian inference with Stan: A tutorial on adding custom distributions. Behavior research methods. 2017;49:863-86.

[30] Guide 98-3/Suppl.1, Uncertainty of measurement-Part 3: Guide to the expression of uncertainty in measurement (GUM: 1995)-Supplement 1: Propagation of distributions using a Monte Carlo method: ISO/IEC; 2008.

[31] Tian W, Yang S, Li Z, Wei S, Pan W, Liu Y. Identifying informative energy data in Bayesian calibration of building energy models. Energy and Buildings. 2016;119:363-76.

[32] Chong A, Menberg K. Guidelines for the Bayesian calibration of building energy models. Energy and Buildings. 2018;174:527-47.

[33] Hoffman MD, Gelman A. The No-U-Turn Sampler: Adaptively Setting Path Lengths in Hamiltonian Monte Carlo. Journal of Machine Learning Research. 2014;15:1593-623.

[34] Ma ZJ, Wang SW. An optimal control strategy for complex building central chilled water systems for practical and real-time applications. Building and Environment. 2009;44:1188-98.

[35] Ma ZJ, Wang SW. Supervisory and optimal control of central chiller plants using simplified adaptive models and genetic algorithm. Applied Energy. 2011;88:198-211.

[36] Kang J, Wang SW, Gang WJ. Performance of distributed energy systems in buildings in cooling dominated regions and the impacts of energy policies. Applied Thermal Engineering. 2017;127:281-91.

[37] Minasny B, McBratney AB. A conditioned Latin hypercube method for sampling in the presence of ancillary information. Computers & Geosciences. 2006;32:1378-88.

[38] Minasny B, McBratney A. Conditioned Latin hypercube sampling for calibrating soil sensor data to soil properties. Proximal soil sensing: Springer; 2010. p. 111-9.